Nanoscale

Accepted Manuscript

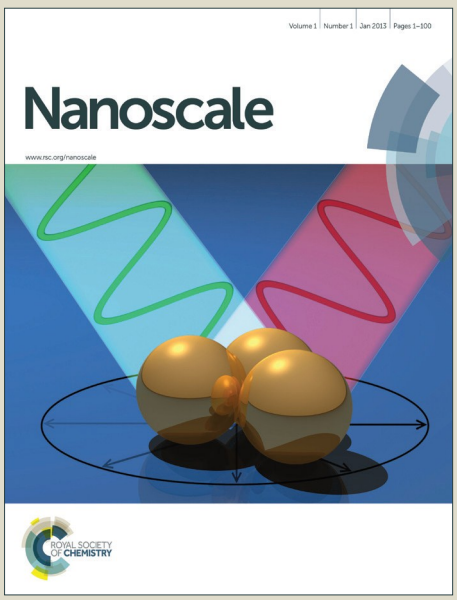

ROYAL SOCIETY OF CHEMISTRY

www.rsc.org/nanoscale

Journal Name

ARTICLE

Simultaneous determination of indoor ammonia pollutionand its biological metabolite in human body by use of a recyclable nanocrystalline lanthanide functionalized MOF

Received 00th January 20xx,
Accepted 00th January 20xx

DOI: 10.1039/x0xx00000x

www.rsc.org/

Ji-Na Hao and Bing Yan*

A Eu^{3+} post-functionalized metal-organic framework of Ga(OH)bpydc(Eu^{3+}@Ga(OH)bpydc, **1a**)with nano-size and intense luminescence is successfully synthesized and characterized. Luminescence explorations revealthat **1a** can selectively and sensitively detect ammonia gas among various indoor air pollutants. More importantly, **1a** can simultaneously realize the determination of the biological metabolite of ammonia in human body (urinary urea), which represents a rare example in reported luminescent senor that can realize pollutants' both environmental monitoring and biological indicators' detection. What' more, as a sensor for both, **1a** also exhibits several appealing features including high selectivity and sensitivity, fast response, simple and quick regeneration, and excellent recyclability.

Introduction

It was reported that for a person about 70 % − 90 % of the time was spent in indoors environment,[1] therefore, the indoor air quality has great effect on people's health. The World Health Organization estimates that nearly two million people die prematurely each year from indoor air pollution (IAP).[2]Recently,IAP is gaining more and more attention with the improvement of living standard and indoor decoration gradually becoming popular. Among the numerous indoor air pollutants, formaldehyde, ammonia, and benzene are the most representatives, which come from the furnishings and decorating materials.[3] Of the three gases, ammonia (NH_3) has higher over-standard rate and ranks highest in the indoor air pollution.[4] Such a colorless, volatile and corrosive gas with a pungent odor is toxic and harmful to humans' health. It irritates eyes, noses, throats, respiratory tracts as well as skins of humans, which can lead to vomiting, headaches, pneumonedema, respiratory disease, permanent blindness and even death.[5] In order to protect people from excessive ammonia exposure, the American National Institute for Occupational Safety and Health (NIOSH) has stipulated the immediately dangerous to life or health concentration (IDLH) of ammonia to be 300 ppm, and the Occupational safety and Health Administration (OSHA) has regulated the threshold limit value of ammonia in the work place as 50 ppm.[6] Therefore, for the health and safety of human, it became highly necessary to design and fabricate a long-term reliable, highly sensitive, miniaturized, room-temperature efficient, and no-humidity impact ammonia gas sensor, which can detect and monitor indoor NH_3 concentration in real time. However, because of the heterogeneous factors of individuals, only monitoring the environmental ammonia level does not pretty accurately estimate people's real intoxication level. As we all know, the main outlet of inhaled ammonia in human body is synthesis of urea in liver and excreted in the urine. What's more, researches have shown that exposure to 13 mg/m^3 ammonia for 8 h will lead to the increase of urea content in human urine. Therefore, besides monitoring indoor ammonia, it is also necessary to determine the concentration of ammonia's metabolite (urinary urea) in human body by the probe to comprehensively reflect the real ammonia exposure and intoxication of human beings.

Various types of analytical methods have been exploited for the detection of ammonia,[7] in which the fluorescent chemosensor is an expedient detection device because it has many advantages over other methods such as a high signal output, simple detection, low cost, and reliability. Among various fluorescent materials, Lanthanide functionalized metal-organic frameworks (Ln-MOFs) have been widely used as sensing materials due to the excellent luminescence and accessible porosity within such materials. To date, many fluorescent probes based on Ln-MOFs have been successfully developed, and these probes were mainly investigated for the detection of cations,[8] anions,[9] small molecules,[10] and nitroaromatic explosives.[11] Nevertheless, to our best knowledge, Ln-MOFs as luminescent sensors for both ammonia and its metabolite (urinary urea) have never been reported. What's more, considering the efficiency of a sensor in practical applications, the sensor also needs to meet the following requirements: high selectivity and sensitivity, fast

[a] Shanghai Key Lab of Chemical Assessment and Sustainability,Department of Chemistry, Tongji University, Siping Road 1239, Shanghai 200092, China. E-mail: byan@tongji.edu.cn;

†Electronic Supplementary Information (ESI) available: Experimental section; XPS spectra; N2 adsorption-desorption isotherms; ICP data; SEM image; PXRD patterns and other luminescence data. See DOI: 10.1039/x0xx00000x

response, good reversibility or regenerability, and facile nanocrystallization of MOFs materials in order to easily fabricate devices with luminescent sensing functions. In particular, the latter two requirements are still challenging for the florescent probes, and few examples have been reported. However, in this work, the developed luminescent sensor for both ammonia and urea based on a lanthanide-functionalized MOF could completely fulfil the above-mentioned factors. The fluorescent sensor wasfabricated by simply immobilization of europium salts on the framework of Ga(OH)(bpydc) via coordination to the accessible 2,2′-bipyridine sites on the linker molecule.

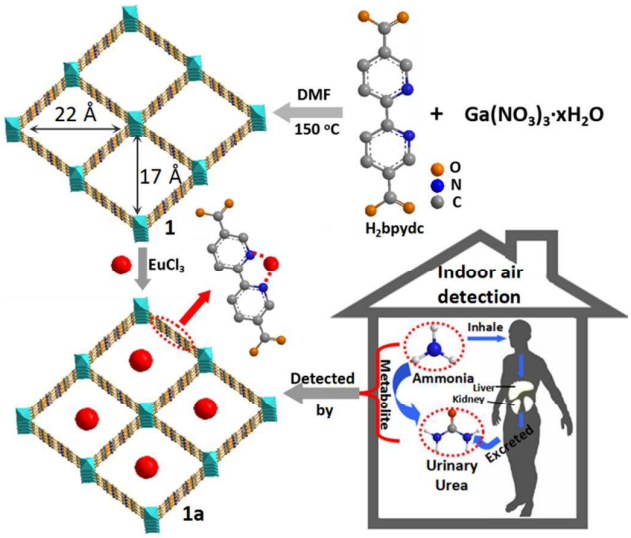

Scheme 1 Schematic representation of synthesis route ofnanocrystal**1a** as a fluorescent sensor for indoor ammonia and its biological metabolite (urinary urea) in human body.

Results and discussion

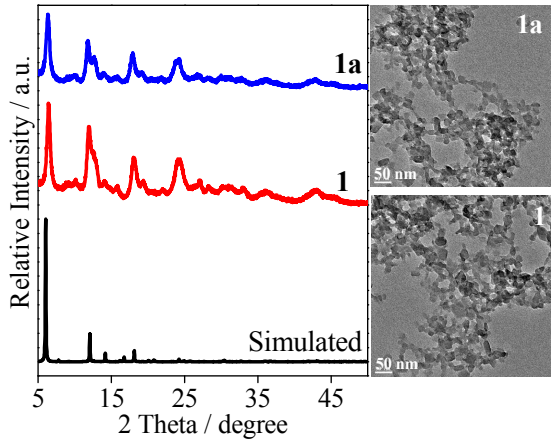

Figure 1 PXRD patterns of simulated **1**, as-synthesized**1**, and **1a**; and TEM images of **1** and **1a**.

Reactions of H_2bpydc with $Ga(NO_3)\cdot xH_2O$ in DMF at 150 °C for 48 h afforded Ga(OH)(bpydc) (**1**) as an orange nano-crystalline solid (Scheme 1).[12] Good agreement between the simulated and experimental PXRD patterns verifies the formation of the pure phase of **1** (Figure 1). TEM studies (Figure 1) have demonstrated that the obtained product is in the nanoscale range consisting of irregularly shaped, crystalline nanoplates with fairly uniform sizes of approximately 30−50 nm. The structure of **1** is built of infinite, one-dimensional chains of octahedral $GaO_4(OH)_2$ units that connects via bpydc linkers to give a 3D open framework with rhombic-shaped pores (22×17Å, Scheme 1). Importantly, **1** has accessible 2,2′-bipyridine units in its framework which allows for its coordination to Ln^{3+} cations to develop fluorescent materials. The as-synthesized**1** was activated and then soaked in an ethanol solution of $EuCl_3\cdot 6H_2O$ to afford Eu^{3+}@**1** (**1a**). The coordination of Eu^{3+} to the free N,N-chelating sites in **1** wasconfirmed by the N 1s spectra shown in Figure S1, which indicated a higher binding energy for the N1S peak of **1a** (398 eV) compared to the pristine **1** (397 eV).[9e,13]Themolar ratio of Eu/Ga in **1a**was measured to be 0.08 by ICP-MS analysis (Table S1). The successful Eu^{3+} loading does not influence the crystalline integrity and morphology of **1**, as demonstrated by PXRD and TEMin Figure 1. The permanent porosity of the de-solvated **1** and **1a** was analyzed by N_2 adsorption-desorption experiments at 77 K (Figure S2). The BET surface areas of **1** and **1a** were calculated to be 541 and 393 $m^2\cdot g^{-1}$, respectively. The reduced surface area of **1a** is attributed to partial blocking of the open pores in **1** by Eu^{3+} cations.[14]

Solid-state luminescent properties of **1** and **1a**were investigated at room temperature. As shown in Figure S3a, a strong emission band at 537 nm emerges in **1** when excited at 400 nm. After incorporating Eu^{3+} cations, the emission band of the framework is significantly suppressed (Figure S3b),instead, the typical narrow-band emissions of Eu^{3+} cations appear at 579, 592, 614, 649, and 695 nm, corresponding to the $^5D_0\rightarrow{}^7F_J$ (J=0-4) transitions, respectively. This indicates that the Eu^{3+} cations not only be successfully encapsulated inside the channels of **1** but also be effectively sensitized by **1**. Under an irradiation of a UV lamp, the **1a** samples emitted bright red color (inset of Figure S3b), which can be readily observed by naked eyes as a qualitative indication of Eu sensitization by **1**. These results indicate that compound **1** can serve as both a host and an antenna for protecting and sensitizing extra-framework Eu^{3+} emitting that are encapsulated within the MOF pores.

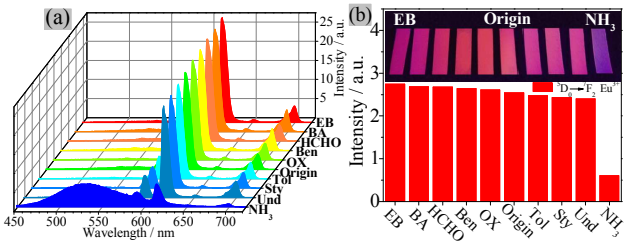

Figure 2(a) PL spectra of **1a** film after exposing to various indoor gas pollutants for 1h; (b) the relative emission intensities at 614 nm. (λ_{ex} = 338 nm), the inset shows the corresponding photographs under 365 nmUV-light irradiation.

The permanent porosity and efficient solid-state emission of **1a** encouraged us to examine its ability to sense indoor air pollutants, mainly including formaldehyde (HCHO),benzene(Ben), ammonia (NH_3), and TVOC (benzene, toluene (Tol), o-Xylene (OX), ethylbenzene (EB), styrene (Sty), butyl acetate (BA), n-undecane (Und)). A nanoscale **1a** film fabricated by spin-coating which is smooth and continuous (SEM image inFigure S4a) was used to evaluate the sensing performance. The **1a** film device was exposed tovarious vapors of the aforementioned indoor air pollutantsfor 1h, and it maintains a stable framework after adsorbing various gas,as revealed by the almost same PXRD patternsshown in Figure S4b. The solid-state luminescent measurements were recorded andcompared in Figure 2. Interestingly, most organic vapors have a negligible effect on the luminescence of**1a** film, except in the case of NH_3, which induce a remarkable reduction (76 %) of luminescence intensity of Eu^{3+} at 614 nm. In accordance with the change in fluorescence spectra, under the irradiation of a UV lamp, only the **1a** film absorbed NH_3 shows a significantly darker luminescence than that from the original one(inset of Figure 2b), which could be distinguished easily by naked eyes. The different effects on the emission between NH_3 and other vapors are clearly observed, indicative of the fact that Eu^{3+}@**1** film can be considered as a promising luminescent probe for NH_3.

Achieving high selectivity toward NH_3 over the other competitive species coexisting is a very important feature to evaluate the performance of the sensor. Therefore, the competition experiments were also conducted. The sensing film was exposed to the mixture of $NH_3{\cdot}H_2O$ and the other vapors for 1 h, respectively, and then the emission spectra were measured. As shown in Figure S5a, the emission spectra displayed a similar pattern at 614 nm to that with NH_3 only. This indicates that the quenching effect of NH_3 on the emission of **1a** film is not influenced by the coexisting gas pollutants, further validating the excellent selectivity of the sensor towards NH_3.

Sensitivity is another key factor in evaluating a probe. To investigate the detection limit of the sensor for NH_3, **1a**film was exposed to various concentrations of ammonia gasesat room temperature and then the changes in the luminescence intensity at 614 nm was recorded in Figure 3a. It is observed that the quenching efficiency (QE = $(1 - I/I_0) \times 100$ %) graduallyincreased with rising NH_3gas concentration,and a good linear relationship (R^2 = 0.991) between QE and the concentration of ammonia is detected over the range from 10 to 500 ppm.According to the 3σ IUPAC criteria[15] and the fitted plot ($1 - I/I_0 = 0.1544 + 1.52\times10^{-3}C$),the detection limit of the sensor was extrapolated to be 2.4 ppm, which is much lower than the threshold limit value of 50 ppm in the workplace and the IDLH concentration of 300 ppm.

In order to test the response rate of **1a** film as gas sensor, the real-time sensing of NH_3vapors was implemented by using the film device placed in a home-made setup (see experimental section), and the time-dependent fluorescence quenching profile were obtained in Figure3b. The results show that the luminescence intensity of the film is significantly reduced, even if it is exposed to NH_3 vapors for 30 s. Within 240 s, the luminescence quenching reaches a maximum with a quenching percentage of more than 70 %. This demonstrates a very fast luminescence response of the sensor to NH_3. Repeatability for a sensory material is a very important parameter to assess the sensor's practicability. After detection of NH_3, the luminescence intensity of the film gradually returned to its initial value after exposure to ambient air for 10 min (Figure 3c), due to the volatilization of NH_3. And the regeneration time of **1a**/NH_3 can be further shortened by heating treatment. Only 5 min and 3 min were required for **1a**/NH_3 to recover their fluorescence intensity to that of the naked **1a** when they were treated at 40 °C and 80 °C, respectively (Figure S5c,d). This is because heating can accelerate the volatilization of NH_3. The recovered film was reused in the next cycle and showed analogous changes. The results are presented in Figure 3d and S5b. It is observed that the luminescent intensity and PXRD of the film after three recycles are well consistent with that of the original one, implying that the film can recover well and can repeatedly detect NH_3. Importantly, the regeneration of NH_3 probe is completed in air and at room temperature, without needing heating or vacuum methods, which can save energy and costs.

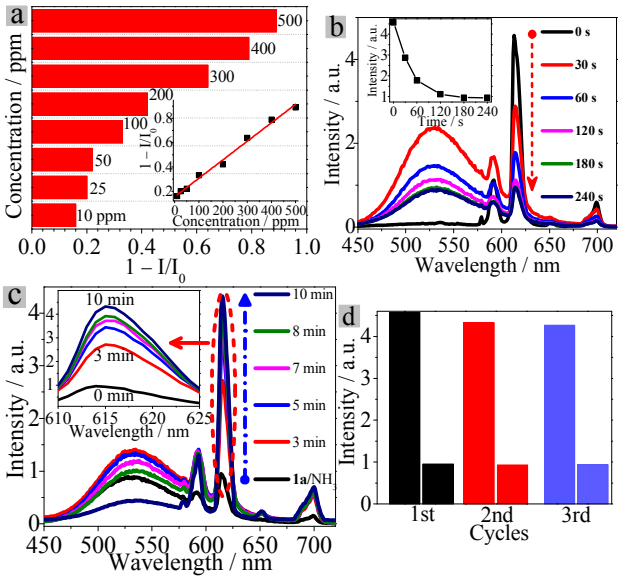

Figure 3 a)Comparison of the luminescence intensity of**1a**film at 614 nm exposed to various ammonia concentrations and the plot of $1\text{-}I/I_0$ versus NH_3 concentration in the inset; b) Emission spectra of **1a** film upon exposed to NH_3 vapors at various time intervals (λ_{ex} = 338 nm) and the emission intensity at 614 nm as a function of exposure time in the inset; c) the luminescence response of **1a** film sensor absorbed ammonia after exposing to ambient air for different time (inset is the amplifying image); d) three consecutive quenching and regenerating cycles.

From the foregoing discussion, we can conclude that **1a** film could act as a highly selective and sensitive probe for ammonia. More importantly, **1a** also realized the determination of the biological metabolite (urinary urea) of inhaled ammonia gas in human body. The joint determination of indoor environmental ammonia and urinary urea in human body could comprehensively reflect the real ammonia exposure and intoxication of human beings.

In chemistry, urine could be defined as water solutions containing various chemicals, mainly including creatinine (Cre),

creatine, urea, uric acid (UA), hippuric acid (HA), SO_4^{2-}, Na^+, K^+, NH_4^+,Cl^- or glucose (Glu). To be a qualified sensor for urine ingredients, water toleration is essential to the sensor. Therefore, its stability in water was primarily investigated. As shown by the PXRD in Figure 6A, after immersing in water for 16 h**, 1a**maintains its framework well. Besides, **1a** also exhibits good photostability in aqueous solutions. As evidenced by Figure 6B, the luminescence intensity of **1a** shows little reduction after several days' storage in water. These results demonstrate that **1a** is competent for a fluorescence sensorof urine components. Urinalysis, essentially, is the detection of the above-mentioned chemicals. Therefore, **1a** powders were dispersed in the aqueous solutions of these various chemicals, respectively, and PXRD patterns (Figure S7) confirm it is insoluble and stable in these solutions. The suspension-state fluorescent measurements were depicted in Figure 4a. Notably, only urea induced a2-fold enhancement in the emission intensity of **1a** at 614 nm, while nearly no fluorescence intensity changes were observed in the presence of others. This indicates **1a**could selectively recognize urea in aqueous solutions.

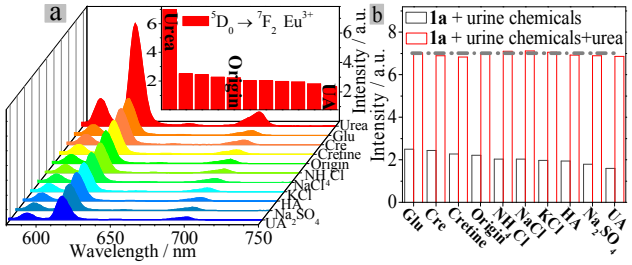

Figure 4(a) Suspension-state PL spectra and the relative intensities of $^5D_0 \rightarrow {}^7F_2$ at 614 nm (inset of a) for **1a** dispersed in various urine chemicals(10^{-2} M, λ_{ex} = 338 nm);(b) Luminescence responses of **1a** (1 mg/mL) upon the addition of urea (0.01 M) in the presence of background of various urine chemicals (0.02 M) in aqueous solution (λ_{ex} = 338 nm).

The interferential experiments were also conducted for **1a** sensor, since these various chemicals are coexisting in urine. Figure 4b shows the fluorescence response of **1a** to urea in the presence of other urine chemicals. The emission intensity enhancement induced by urea was not affected by the coexisting components, further confirming that **1a** is a highly selective probe for urea.

In order to quantitatively describe the relationship between the enhancing efficiency and the concentration, the responses of the sensor to increasing urea concentration were investigated, as illustrated in Figure 5a and 5b. It is observed that the fluorescence intensity **1a** at 614 nm increased linearly with the concentration of urea in the range of 0.6 −50 mg/mL (I/I_0= 3.355 + 1.019 lg[Urea], R^2=0.989). Urea can be directly detected at concentrations as low as 0.6 mg/mL, which is sufficient for detection of millimolar concentrations of urea in urine.

Fast response and simple recovery are important parameter for a desired sensor. We therefore tested the response rate and regenerated ability of **1a** sensor for urea. Figure 5c demonstrates that **1a** shows a very rapid and evident response to urea in aqueous solutions. Within 5 min, the luminescence increase was almostmaximum. The **1a**sensor for urea could also be regenerated and reused by centrifuging the dispersed powder in urea aqueous solutions and washing with water for several times. As demonstrated by Figure S8a, after the fluorescence enhancement induced by urea, the following water washing for three times could make the emission intensity almost recovers to the level before urea addition. Moreover, after five consecutive cycles of enhancing and recovery, the luminescent intensity of **1a** in water is comparable to the initial state (Figure 5d). The unchanged PXRD of **1a** after five runs of recycling (Figure S8b) suggests its framework still remains intact. These confirm the good reusability of the sensor for urea.

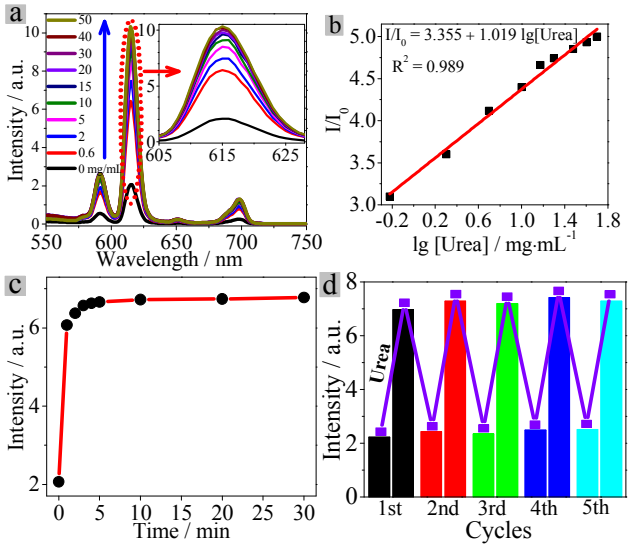

Figure 5(a) Luminescence spectra of **1a** under different concentrations of urea aqueous solution (λ_{ex} = 338 nm), and b) the luminescence intensity ratio I/I_0*vs.*the logarithm of the urea concentration plot; c) variation of fluorescence intensity of **1a** at 614 nm with immersion time in aqueous solution of urea (10^{-2}M);d) the regeneration cycles of **1a** sensor used in detecting urea.

The excellent performances of the sensor for urea in aqueous solutions encourage us to further evaluate its analytical efficiency in practical applications. Here, a series of human urine specimens, spiked with different concentrations of urea were regularly analyzed. As summarized in Table S2, all the obtained recoveriesare more than93 %, suggesting that this method was practicable for the detection of urea in human urine. By six repeated determination of urea in urine specimens utilizing this sensor, the resulting relative standard deviation (RSD) was found to be less than 4 %, further validating the reliability and accuracy of the proposed method.

We tentatively explored the mechanism of the luminescence response to ammonia and urea. The discussions were given as follows: (1) The identical PXRDof NH_3-**1a** or urea-**1a** with **1a** proves that the framework of **1a**remained intact and the luminescence quenching or enhancing was not caused by the transformation of crystallization structure; (2) The emission lifetimes of **1a** in the absence and presence of ammonia or urea were measured and remained almost unchanged (Figure S9), suggesting that there are no interactions between ammonia or urea and the Eu^{3+} ions,[16] and changes in the emission intensity are related to the interactions

between ammonia or urea and the ligands bpydc; (3) As a sensor for both ammonia and urea, **1a** can be simply and quickly regenerated, indicating that the interactions between ammonia or urea and the ligands are weak forces such as hydrogen bonds.As proved by Figure S10a, after exposure to NH_3, the IR absorption peaks belonging to the skeleton vibration of 2'2-bipyridine rings shifted from 1410 cm^{-1} and 859 cm^{-1} to 1400 cm^{-1} and 845 cm^{-1}, respectively, and the absorption intensity at 1400 cm^{-1} had an obvious enhancement.This evidences the existence of the hydrogen bonds between **1a** and ammonia.[17]The UV-Vis absorption peak of **1a**in Figure S10balso shows a blueshift (~14 nm) with the presence of NH_3, further demonstrating the formation of the hydrogen bonds between the 1a and NH_3.Urea also induces the similar changes of IR and UV-Vis absorption(Figure S11), indicating the hydrogen-bonding interactions between urea and ligands.Therefore, we speculate that the hydrogen bonds between ammonia or urea and ligands affect the energy transfer efficiency from ligand to Eu^{3+} ions since the luminescence intensity of Ln^{3+} crucially depends on the efficiency of ligand to Ln energy transfer (Scheme S1a).[18]As shown in Figure S12a, with the presence of ammonia, the ligands' emission has a bathochromic shift of 24 nm, indicating a decrease of the π* energy level of the ligands by the hydrogen bonds. This decrease of the ligands' π* energy level block the pathway of energy transfer from π*to Ln states, localizing the emission on the ligand (Scheme S1b).[19] As a result, the LC-emission in **1a** after exposure to ammonia increased and the Eu-luminescence significantly decreased (Figure S13a).On the contrary, urea induces a hypochromatic shift (27 nm) in the emission of the ligands (Figure S12b), demonstrating an increase energy level of the π* orbits of the ligands by the hydrogen bonds. This make the energy gap between the ligands' π* and Ln's emitting state matching more appropriate and facilitate energy transfer process of ligand-to-Ln (Scheme S1c). Therefore, with the presence of urea, **1a** only show an enhanced luminescence of the Ln without any that of the **1a**'s ligands (Figure S13b).In conclusion, the sensing mechanism of **1a** for ammonia or urea is based on their hydrogen bonds interaction with 1a's ligands, which changes the excited stated energy level of ligands, thus affects the ligand-to-Ln energy transfer efficiency, and consequently leads to different luminescent emission.

Conclusions

A europium-functionalized MOF with nano-size and excellent luminescence has been successfully synthesized and characterized. This luminescent Ln-MOF material not only shows significant selective quenching response for ammonia among various indoor air pollutants, but also exhibits high selectivity for urea in human urine which is the main biological metabolite of ammonia inhaled by the body. For the determination of ammonia which is an important indoor air pollutant, a film device close to those used in practical applications based on the nano-sized**1a** was easily fabricated, and the luminescent film sensor shows several appealing features including high selectivity (76 % reduction), excellent sensitivity (detection limit, 2.4 ppm), very fast response (~ 30 s), quick regeneration with zero cost, and nanocrystallization. Such goodperformances of the sensing film devices pave an avenue toward low-cost, fast, and potable noses for environmental monitoring of ammonia. As a fluorescent sensor for urea, **1a** also exhibits high selectivity and sensitivity for urea in aqueous solution, short response time (< 5 min) and excellent recyclability, which makes it successfully apply to determination of urea in human urine with recoveries in the range of 93 –104 %. This indicates its promising potential for point-of-care (POC) diagnosis of urinary urea in people exposed to ammonia. This work represents the first example of MOF-based luminescent probes forsimultaneous detection of ammonia gas and its biological metabolite in human body, which realizes the pollutant's both environmental exposure monitoring and biological indicators' detection to accurately estimate the exposed individuals' intoxication. This is significant for air quality control and humanbody health.

Acknowledgements

This work is supported by the National Natural Science Foundation of China (21571142), Developing Science Funds of Tongji University and Science & Technology Commission of Shanghai Municipality (14DZ2261100).

Notes and references

1 C. B. Chang, *Environ. Chem.*, 2015, **35**, 817-823.
2 E. Carter, C. M. Earnest, E. T. Gall, B. Stephens, *Indoor Air*, 2012,**22**,1-2.
3 S. J. Wang, H. Yu and X. X. Cheng, *J. Chem.*, 2014, **2014**, 1-5.
4 C. S. Zheng, P. Zhang, J. Q. Wang, Z. L. Jing, N. Yang and Q. L. Deng, *Occupation and health*, 2004, **20**, 34-35.
5 a) D. C. M.Licyayo, A. Suzuki, M. Matsumoto, *Mycoscience*, 2007, **48**, 20−28; b) Y. Wang, Q. Mu, G. Wang and Z. Zhou, *Sensor Actuat. B-Chem*,2010, **145**, 847-853.
6 X. Liu, N. Chen, B. Q. Han, X. C. Xiao, G. Chen, I. Djerdj and Y. D. Wang, *Nanoscale*, 2015, **7,** 14872-14880.
7 B. Timmer, W. Olthuis and A. van den Berga, *Sensor Actuat. B-Chem*, 2005, **107**, 666-677; b) J. Wang, P. Yang and X. W. Wei, *ACS Appl. Mater. Interfaces*, 2015, **7**, 3816−3824; b) X. F. Yu, Y. C. Li, J. B. Cheng, Z. B. Liu, Q. Z. Li, W. Z. Li, X. Yang and B. Xiao, *ACS Appl. Mater. Interfaces*, 2015, **7**, 13707−13713; c) S. L. Bai, Y. B. Zhao, J. H. Sun, Y. Tian, R. X. Luo, D. Q. Li and A. F. Chen, *Chem. Commun.*, 2015, **51**, 7524-7527.
8 a) H. Xu, H. C. Hu, C. S. Cao and B. Zhao, *Inorg. Chem.*, 2015, **54**, 4585-4587; b) J. N. Hao and B. Yan, *J. Mater. Chem. C*, 2014, **2**, 6758-6764; c) B. Liu, W. P. Wu, L. Hou, Y. Y. Wang, *Chem. Commun.*, 2014, **50**, 8731-8734; d) J. N. Hao and B. Yan, *Chem. Commun.*, 2015, **51**, 7737-7740; e) Q. Tang, S. Liu, Y. Liu, J. Miao, S. Li, L. Zhang, Z. Shi and Z. Zheng,*Inorg. Chem.*, 2013, **52**, 2799-2801; f) Y. M. Zhu, C. H. Zeng, T. S. Chu, H. M. Wang, Y. Y. Yang, Y. X. Tong, C. Y. Su and W. T. Wong, *J. Mater. Chem. A*, 2013, **1**, 11312-11319; g) J. N. Hao and B. Yan, *J. Mater. Chem. A*, 2015, **3**, 4788-4792; h) B. L. Chen, L. B. Wang, Y. Q. Xiao, F. R. Fronczek, M. Xue, Y. J. Cui and G. D. Qian, *Angew. Chem. Int. Ed.*, 2009, **48**, 500-503; i) W. T. Yang, Z. Q. Bai, W. Q. Shi, L. Y. Yuan, T. Tian, Z. F. Chai, H. Wang and Z. M. Sun, *Chem. Commun.*, 2013, **49**, 10415-10417.
9 a) F. Y. Yi, J. P. Li, D. Wu and Z. M. Sun, *Chem. Eur.J.*, 2015, **21**,11475 –11482; b) H. P. Liu, H. M. Wang, T. S. Chu, M. H. Yu, Y. Y. Yang, *J. Mater. Chem. C*, 2014, **2**, 8683-8690; c) B. L. Chen, L. B. Wang, F. Zapata, G. D. Qian and E. B. Lobkovsky, *J. Am.Chem. Soc.*, 2008, **130**, 6718-6719; d) J. M. Zhou, W. Shi, N. Xu and P. Cheng, *Inorg. Chem.*, 2013, **52**, 8082-8090; e) J.

M. Zhou, W. Shi, H. M. Li, H. Li and P. Cheng, *J. Phys. Chem. C*, 2014, **118**, 416-426; f) H. Xu, C. S. Cao and B. Zhao, *Chem. Commun.*, 2015,**51**, 10280-10283; g) P. F. Shi, H. C. Hu, Z. Y. Zhang, G. Xiong and B. Zhao, *Chem. Commun.*, 2015, **51**, 3985-3988.

10 a) X. Q. Wang, L. L. Zhang, J. Yang, F. L. Liu, F. N. Dai, R. M. Wang and D. F. Sun, *J. Mater. Chem. A*, 2015, **3**, 12777-12785; b) S. N. Zhao, X. Z. Song, M. Zhu, X. Meng, L. L. Wu, J. Feng, S. Y. Song and H. J. Zhang, *Chem. Eur. J.*, 2015, **21**, 9748-9752; c) Y. L. Hou, H. Xu, R. R. Cheng and B. Zhao, *Chem. Commun.*, 2015, **51**, 6769-6772; d) Y. Li, S. S. Zhang and D. T. Song, *Angew. Chem. Int. Ed.*, 2013, **52**, 710-713; e) B. L. Chen, Y. Yang, F. Zapata, G. N. Lin, G. D. Qian and E. B. Lobkovsky, *Adv. Mater.*, 2007, **19**, 1693-1696; f) Z. Y. Guo, H. Xu, S. Q. Su, J. F. Cai, S. Dang, S. C. Xiang, G. D. Qian, H. J. Zhang, M. O'Keeffe and B. L. Chen, *Chem. Commun.*, 2011, **47**, 5551-5553.

11 a) J. H. Qin, B. Ma, X. F. Liu, H. L. Lu, X. Y. Dong, S. Q. Zang and H. W. Hou, *Dalton Trans*., 2015, **44**, 14594-14603; b) W. Xie, S. R. Zhang, D. Y. Du, J. S. Qin, S. J. Bao, J. Li, Z. M. Su, W. W. He, Q. Fu and Y. Q. Lan, *Inorg. Chem.*, 2015, **54**, 3290-3296; c) S. B. Ding, W. Wang, L. G. Qiu, Y. P. Yuan, F. M. Peng, X. Jiang, A. J. Xie, Y. H. Shen and J. F. Zhu, *Mater. Lett.*, 2011, **65**, 1385-1387.

12 Y. Y. Liu, K. Leus, T. Bogaerts, K. Hemelsoet, E. Bruneel, V. Van Speybroeck and P. Van Der Voort, *ChemCatChem*, 2013, **5**, 3657-3664.

13 a) Y. Lu, B. Yan and J. L. Liu, *Chem. Commun.*, 2014, **50**, 9969-9972; b) L. Y. Chen, Z. Q. Gao and Y. W. Li, *Catal. Today*, 2015, **245**, 122-128; c) Z. M. Hao, X. Z. Song, M. Zhu, X. Meng, S. N. Zhao, S. Q. Su, W. T. Yang, S. Y. Song and H. J. Zhang, *J. Mater. Chem. A*, 2013, **1**, 11043-11050.

14 a) F. Carson, S. Agrawal, M. Gustafsson, A. Bartoszewicz, F. Moraga, X. D. Zouo and B. Martín-Mature, *Chem. Eur. J.*, 2012, **18**, 15337-15344; b) T. H. Zhou, Y. H. Du, A. Borgna, J. D. Hong, Y. B. Wang, J. Y. Han, W. Zhang and R. Xu, *Energy Environ. Sci.*, 2013, **6**, 3229-3234.

15 A. M. Committee, *Analyst*, 1987, **112**, 199-204.

16 a) G. R. Choppin, D. R. Peterman, *Coordin. Chem. Rev.*, 1998, **174**, 283-299; b) X. H. Zhou, L. Li, H. H. Li, A. Li, T. Yang and W. Huang, *Dalton Trans.*, 2013, **42**, 12403-12409.

17 T. Fornaro, D. Burini, M. Biczysko and V. Barone, *J. Phys. Chem. A*, 2015, **119**, 4224-4236.

18 a) N. Arnaud, E. Vaquer and J. Georges, *Analyst*, 1998, **123**, 261-265; b) S. I. Weissman, *J. Chem. Phys.*, 1942, **10**, 214-217.

19 a) M. D. Allendorf, C. A. Bauer, R. K. Bhakta and R. J. T. Houk, *Chem. Soc. Rev.*, 2009, **38**, 1330-1352; b) Y. J. Cui, Y. F. Yue, G. D. Qian and B. L. Chen, *Chem. Rev.*, 2012, **112**, 1126-1162.